The dataset is potentially useful, but the manuscript does not sufficiently demonstrate its added value over existing satellite-based gap-free global soil moisture datasets. The validation is extensive in quantity, but much of it repeatedly compares the final product with other soil moisture datasets or reconstruction methods. Additional evaluation of physically and meteorologically meaningful soil moisture variability is needed before the dataset can be considered reliable for broader Earth system applications.

Re: Thank you very much for your positive comments on our paper. We have carefully considered your comments and revised the paper accordingly. Please see the response below.

Major comments

1. Clarify the novelty and added value of the dataset. As the authors state in the introduction, many satellite-based global soil moisture datasets already exist. In addition, a previous gap-free FY-3B soil moisture dataset has already been developed. Therefore, the authors should clearly explain what new scientific or practical benefit this dataset provides compared with existing global soil moisture products and the previous FY-3B reconstruction dataset.

Re: Thank you very much for this important comment. We will further clarify the methodological advancement and practical value of the proposed model and dataset and add a comparison experiment with existing global SM products. First, compared with the previously developed spatially seamless FY-3B SM dataset based on the TTP model, GSP represents a further methodological advancement by explicitly exploiting both temporal and spatial neighborhood information. While TTP mainly relied on the temporal information of the target pixel, GSP additionally utilizes valid observations in the surrounding spatial neighborhood, allowing more effective use of the spatiotemporal information in FY-3B SM observations. This methodological advancement will be described in greater detail on the Page 5, Lines 175–184. The performance of GSP over TTP is further supported by the validation results in Section 5.2, including both *in-situ* site-level validation and triple-collocation (TC) validation. In addition, Section 5.3 further compares the spatial characteristics of the GSP- and TTP-reconstructed FY-3B SM datasets, with GLDAS-Noah SM introduced as an independent comparison dataset (Page 24, Lines 593–634). The results show that GSP better preserves spatial continuity and local spatial variability than TTP, and retains more detailed spatial structures in the reconstructed FY-3B SM than GLDAS-Noah SM. This further demonstrates the practical value of the reconstruction of FY-3B SM based on GSP. In the revised manuscript, we will further strengthen the discussion of its novelty and value and, to further evaluate its effectiveness, add a comparison experiment with other existing global SM products.

Page 5, Lines 175–184

"Unlike reconstruction methods that mainly exploit temporal information, such as TTP, GSP further incorporates spatial neighborhood information and jointly models local and global spatiotemporal characteristics. To reduce the influence of invalid values in the incomplete FY-3B SM inputs, multi-scale gated convolutions are employed to adaptively extract local spatiotemporal features at different scales. Meanwhile, the residual Swin Transformer captures global spatiotemporal structures through shifted-window self-attention. By integrating these two complementary branches,

GSP can simultaneously suppress the interference of invalid inputs and characterize both local details and global spatial patterns, thereby making more effective use of the available spatiotemporal information in FY-3B SM."

Page 24, Lines 593–634

"*5.3 Spatial comparison among the GSP- and TTP-reconstructed FY-3B SM datasets and GLDAS-Noah SM*

To further examine the spatial characteristics of the reconstructed FY-3B SM dataset, the 25 km GLDAS-Noah SM dataset, which provides spatially complete SM estimates, was introduced as a comparison dataset. Taking the GLDAS-Noah SM dataset and TTP- and GSP-reconstructed FY-3B SM on 16 July 2011 as an example, four lines and six patches were randomly selected for spatial comparison, as shown in Fig. 14. As shown in Fig. 14(b), the TTP-reconstructed FY-3B SM exhibits very limited spatial variation, with locally nearly invariant SM. In contrast, the GSP-reconstructed FY-3B SM shows more pronounced spatial variations. The variation pattern of the difference between GSP and TTP is also generally consistent with that of GSP, indicating that much of the spatial variation between the two reconstructed datasets originates from the spatial variability retained by GSP, whereas the TTP reconstruction tends to produce a more spatially homogeneous distribution. Moreover, the spatial variation patterns of GSP and GLDAS-Noah show broadly consistent fluctuations along several transects. A similar pattern can be observed from the spatial maps in Fig. 14(c). The TTP-reconstructed FY-3B SM exhibits relatively weak spatial texture, whereas the GSP-reconstructed results present more continuous and complete spatial structures while retaining finer spatial details. GLDAS-Noah also reproduces the major large-scale spatial variations, but appears relatively smooth in some regions. This is likely related to the nature of GLDAS-Noah as a land surface model product, for which the spatial distribution is influenced by meteorological forcing, model parameterization, and grid-scale averaging, thereby smoothing part of the local-scale spatial heterogeneity. These comparisons further indicate that, compared with TTP, which primarily considers temporal relationships, GSP can better preserve and reconstruct the spatial structure of the original FY-3B SM by incorporating information from the surrounding spatiotemporal neighborhood. Meanwhile, compared with the model-based GLDAS-Noah dataset, the GSP-reconstructed FY-3B SM based on satellite SM retains more localized spatial details in some regions, reflecting the spatial characteristics inherited from the original satellite observations.

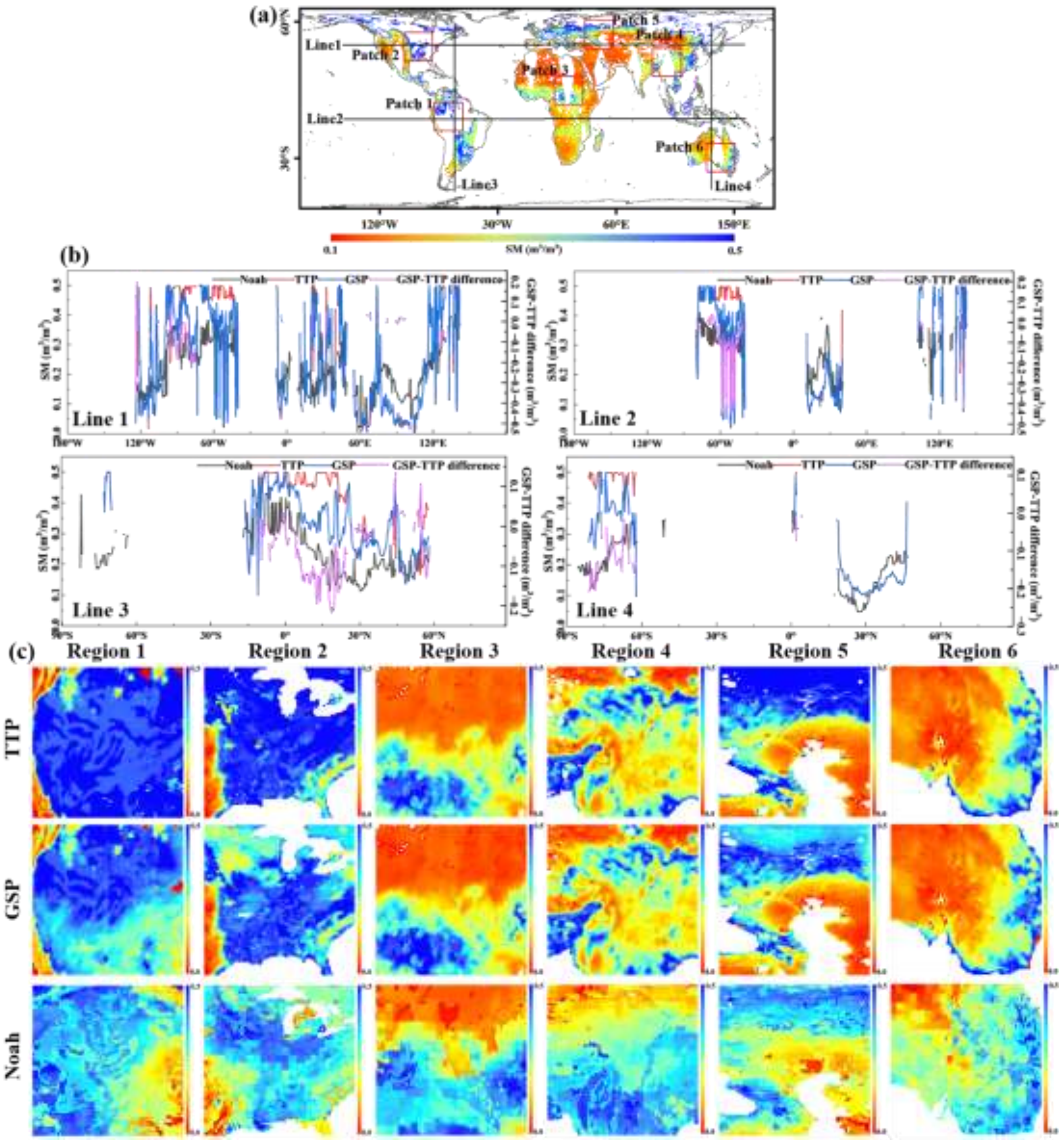

Fig. 14. Comparison of spatial heterogeneity among the TTP-reconstructed FY-3B SM, GSP-reconstructed FY-3B SM, and GLDAS-Noah SM. (a) Locations of six randomly selected patches and four lines at the global scale, where the four lines include two horizontal lines at 41.2485° N and 3.0274° S, and two longitudinal lines at 62.9935° W and 132.2343° E. The center coordinates of the six patches are Region 1 (4.0054° S, 67.4187° W), Region 2 (37.7069° N, 88.2429° W), Region 3 (11.6971° N, 26.2907° E), Region 4 (28.3807° N, 99.1757° E), Region 5 (48.4103° N, 47.1150° E), and Region 6 (28.6028° S, 140.8243° E). (b) Spatial variation profiles of SM along the four lines, comparing TTP-reconstructed FY-3B SM, GSP-reconstructed FY-3B SM, and GLDAS-Noah SM. (c) Visual comparison of the spatial SM patterns of the TTP-reconstructed FY-3B SM, GSP-reconstructed FY-3B SM, and GLDAS-Noah SM for the six selected patches.

2. Limited physical and meteorological validation. The reconstruction is based almost entirely on FY-3B soil moisture itself, without using meteorological forcings or ancillary variables. Also, the use of a four-month temporal mean in the feature fusion step may smooth the reconstructed values

toward the average state. The authors should test whether the final dataset can capture physically meaningful soil moisture variability, such as seasonal variations, wet and dry events, and responses to rainfall/temperature changes.

Re: Thank you very much for this valuable comment. We agree that the physical and meteorological consistency of the reconstructed FY-3B SM dataset should be further evaluated. To address this concern, we will add additional analyses in the revised manuscript. First, to evaluate whether the reconstructed FY-3B SM can capture physically meaningful responses to precipitation events, we have added precipitation variations in Section 4.1 and compared them with the temporal variations of the reconstructed FY-3B SM (Page 14, Lines 435-440, Figs 7-8). Additionally, the in-situ observations and the GSP-reconstructed FY-3B SM time series from 12 July 2011 to 19 August 2019 exhibit generally consistent temporal variations, indicating that the reconstructed dataset preserves the seasonal variability of SM well. From the spatial perspective, we further compared the reconstructed FY-3B SM with precipitation, as shown in Fig. 12. We calculated the monthly mean and standard deviation of both reconstructed FY-3B SM and precipitation. The results show that regions with relatively large temporal variability in reconstructed FY-3B SM are generally spatially consistent with areas exhibiting more active precipitation variability. This spatial correspondence indicates that the reconstructed FY-3B SM is able to reflect hydrologically meaningful wetting and drying variability associated with precipitation. The specific details have been added on Page 24, Lines 546-557. Third, to examine whether the four-month temporal mean used in the feature fusion step causes the reconstructed SM to become overly smoothed toward the mean state, we will further analyze its temporal variability and anomaly characteristics. Specifically, we will compare the temporal standard deviations of the reconstructed and *in-situ* data, and evaluate the anomaly correlation between the reconstructed and *in-situ* data. These analyses will help determine whether the reconstruction preserves meaningful temporal variability and wet/dry anomalies.

Page 14, Lines 435-440

"To further assess whether the reconstructed FY-3B SM based on GSP captures physically meaningful wetting and drying variations, GLDAS-Noah precipitation was introduced in Fig. 7. Across most networks, increases in precipitation are generally accompanied by increases in reconstructed FY-3B SM based on GSP, followed by gradual decreases during subsequent rain-free periods. These results indicate that the reconstructed dataset based on GSP is capable of capturing precipitation events."

Fig. 7

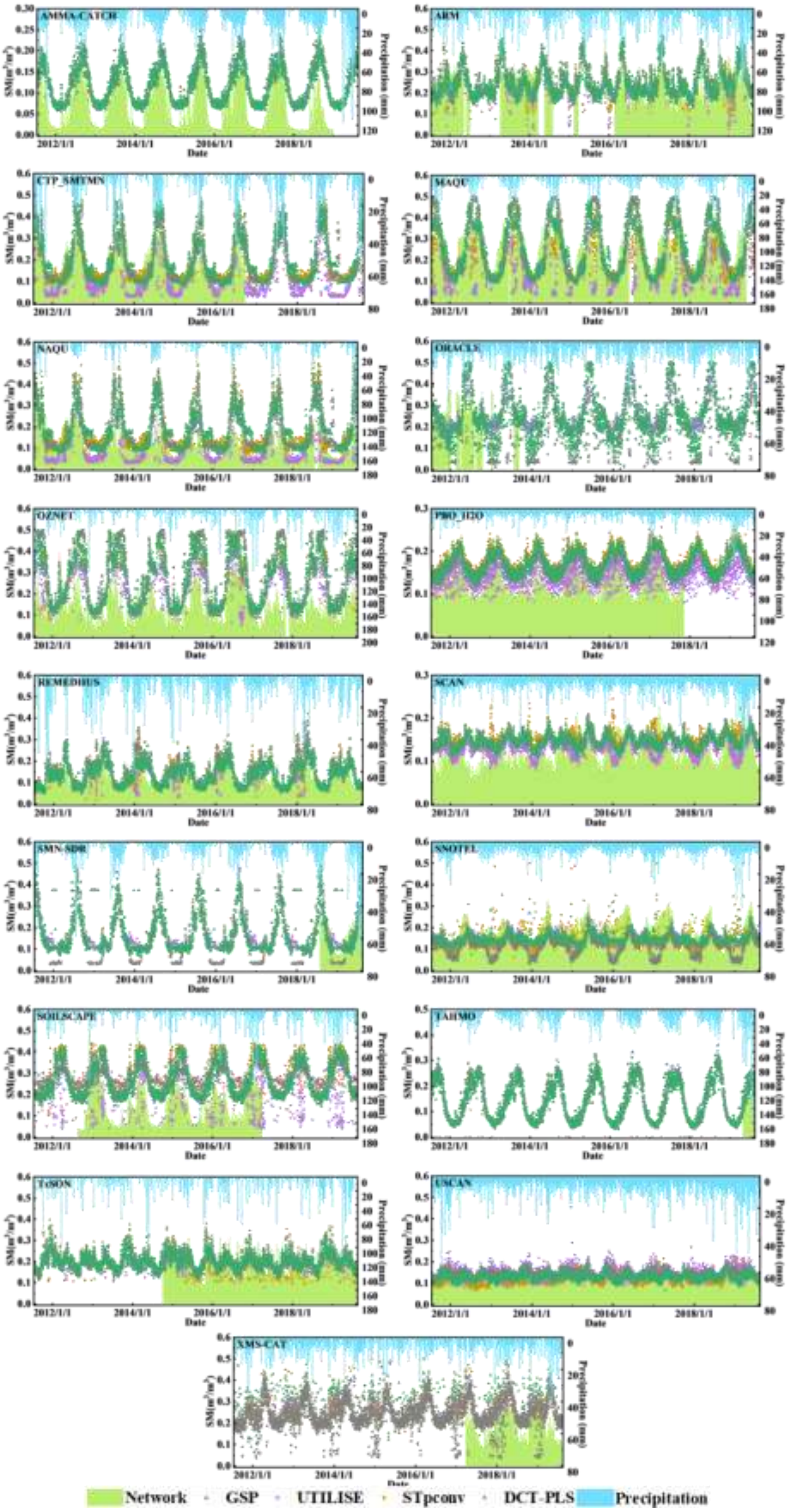

“

Fig. 7. *Temporal profiles of the reconstructed FY-3B SM dataset at the 17 sparse networks,*

with precipitation (the date format on the x-axis is yyyy/mm/dd).

"

Fig. 8

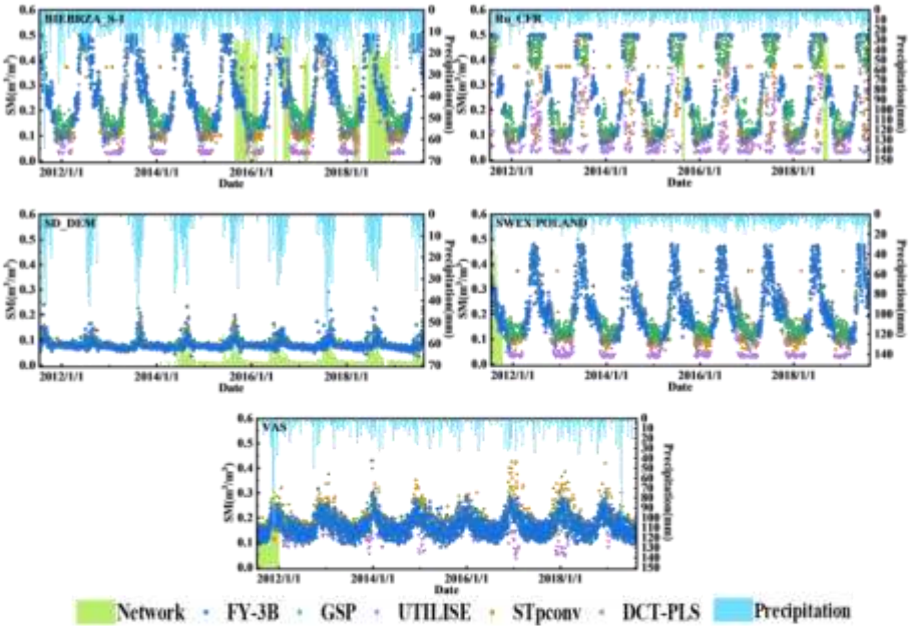

"

Fig. 8. *Temporal profiles of the reconstructed FY-3B SM dataset at the five dense networks, with precipitation (the date format on the x-axis is yyyy/mm/dd).*

"

Page 24, Lines 546-557

"Furthermore, Fig. 12 illustrates the spatial patterns of the reconstructed FY-3B SM and precipitation. (a)–(d) demonstrate that the reconstructed results maintain a consistent spatial structure while exhibiting certain variations, indicating the model's capability to capture continuous daily evolutions. Furthermore, the monthly mean of reconstructed FY-3B SM (Fig. 12 (e)) falls within a physically reasonable range of 0 to 0.5 m^3/m^3, and the standard deviation (Fig. 12 (f)) is constrained within 0 to 0.16 m^3/m^3. These quantitative results demonstrate that the overall spatial configuration remains stable, alongside the presence of localized daily fluctuations. To validate the physical rationale behind the reconstructed FY-3B SM dynamics, we introduced the monthly mean and standard deviation of precipitation for the same period (Fig. 12 (g)–(h)). It is evident that regions with a higher FY-3B SM standard deviation are spatially consistent with active precipitation zones. This consistency confirms that the GSP accurately captures the dynamic hydrological responses."

Fig. 12

“

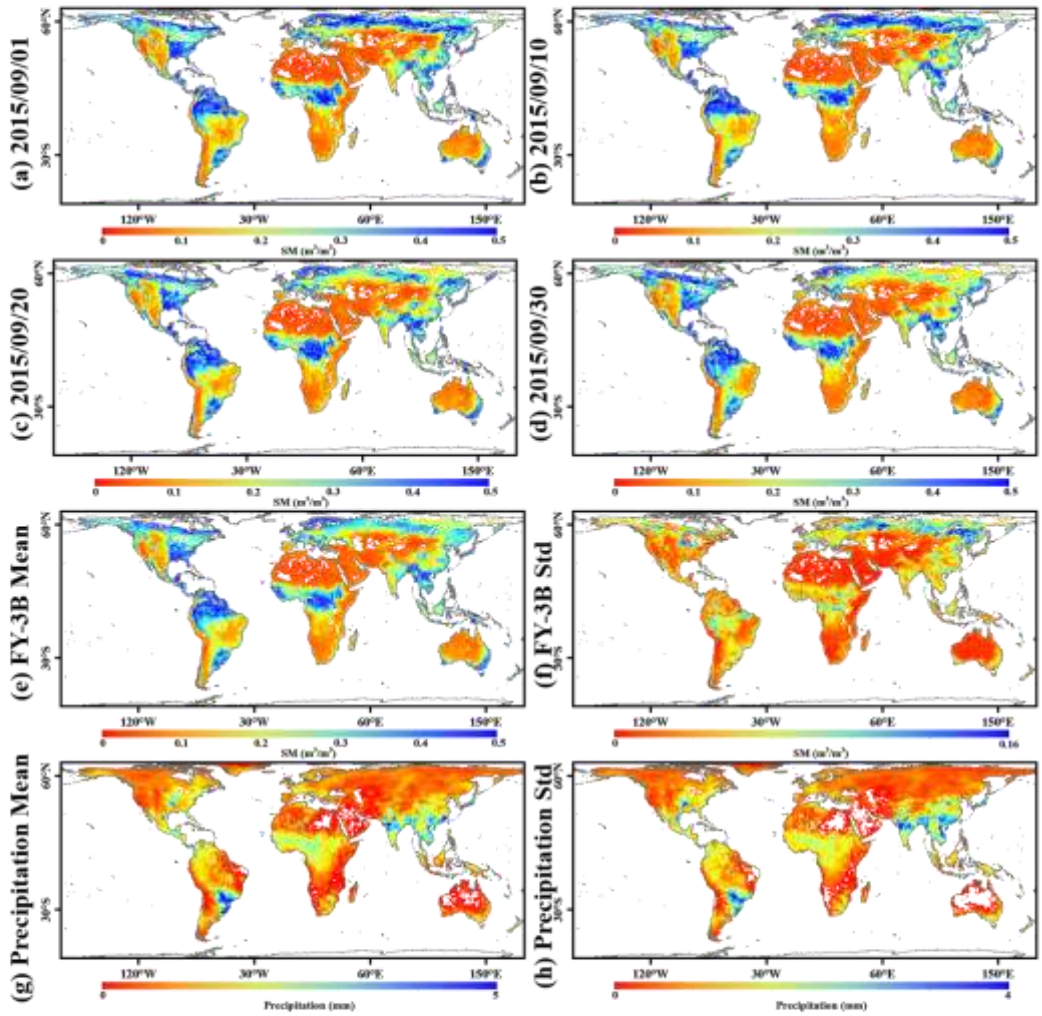

Fig. 12. *Spatial distributions of the reconstructed FY-3B SM and precipitation in September 2015. (a)–(d) present daily reconstructed FY-3B SM on 1 September 2015, 10 September 2015, 20 September 2015, and 30 September 2015, respectively. (e)–(f) present the monthly mean and temporal standard deviation of FY-3B SM for the September 2015. (g)–(h) present the monthly mean and STD of precipitation for the same period.*

”

3. Need for uncertainty information and clearer data limitations. The validation primarily relies on artificial masked FY-3B observations. While this approach is useful, it does not fully prove the accuracy of reconstructed values under real missing-data conditions (e.g. frozen soil, snow, vegetation effects). The final dataset should include uncertainty or quality information, especially to distinguish direct satellite retrievals from reconstructed estimates. Based on this information, the authors should also provide clear guidance for users on data reliability and potential limitations.

Re: Thank you for this important comment. In the revised manuscript, we have therefore further clarified the complementary roles of the simulated-gap and *in-situ* validation experiments, added source information to distinguish original and reconstructed observations, provided information on reconstruction uncertainty, and expanded the discussion of the potential limitations of the dataset.

First, regarding that the validation primarily relies on artificial masking, we would like to clarify that the simulated-gap experiments were designed to reproduce realistic missing-data conditions rather than simply generate random artificial gaps. Specifically, the masks used in the simulated-gap experiments were derived from the actual missing-data patterns corresponding to the testing period observed in the FY-3B SM dataset. These masks preserve the spatial characteristics and distribution patterns of real observational gaps. We have added more details in Page 13, Lines 413-416. Moreover, the simulated-gap experiments can characterize the empirical reconstruction uncertainty under different missing-data conditions. The RMSE were 0.0119, 0.0119, 0.0121, and 0.0121 m^3/m^3 for missing rates of 30–40%, 40–50%, 50–60%, and 60–70%, respectively. These results indicate that the reconstruction error generally increases as the missing rate increases. Therefore, these statistics can be used as references for the expected reconstruction error and data reliability under different missing-data conditions. We emphasize that these values are empirical error estimates derived from simulated-gap experiments and should not be interpreted as strict pixel-level probabilistic uncertainty bounds. Based on these results, we have also added clearer data-use guidance to the Readme.txt and Page 19, Lines 511-513. Users are advised to first distinguish original and reconstructed values using the source flag and to consider the corresponding empirical reconstruction error when using reconstructed estimates.

Second, the network-level *in-situ* validation complements the simulated-gap experiments by providing an independent evaluation under actual missing-data conditions. Specifically, the in-situ observations were used to evaluate reconstructed FY-3B SM at locations corresponding to actual missing satellite observations, rather than artificially masking FY-3B SM. These details have been explicitly added on Page 14, Lines 424-427.

Third, to improve the quality of the final dataset and clearly distinguish direct satellite retrievals from reconstructed estimates, we have added a source flag dataset. This allows users to directly distinguish observations from reconstructed values and prevents the two types of data from being treated as equivalent in subsequent applications. The final dataset has been updated accordingly, and the corresponding description has also been added to the Readme.txt.

Finally, we have expanded the discussion of the potential limitations of the GSP-based reconstruction framework in the revised manuscript. Since GSP relies entirely on the available spatiotemporal information within the FY-3B SM dataset for reconstruction, the availability and representativeness of valid neighboring observations have a substantial influence on reconstruction performance. When missing observations become extensive or spatially/temporally continuous, the amount of effective neighboring information available to constrain the reconstruction is reduced, which may lead to increased reconstruction uncertainty and degraded accuracy. We have explicitly added this limitation to the Page 28, Lines 675-681.

Page 13, Lines 413-416

"Similar to the simulated mask process during training, the real missing patterns from 1 January 2017 to 15 August 2019 in FY-3B SM were applied to simulate partial spatial gaps to evaluate the GSP performance under different proportions of spatial missing (i.e., 30 %-70 %)."

Readme.txt

"## Source flag

A source flag is provided to distinguish background, original, and reconstructed pixels.

0: Background pixels
1: Original FY-3B SM observations
2: Reconstructed FY-3B SM values
Users are advised to use the source flag to distinguish original observations from reconstructed estimates when using the dataset.

Reconstruction uncertainty and data-use guidance
The reconstruction uncertainty was empirically evaluated using simulated-gap experiments based on actual missing-data patterns observed in FY-3B SM.
The RMSE values were 0.0119 m3/m3, 0.0119 m3/m3, 0.0121 m3/m3, and 0.0121 m3/m3 for missing rates of 30–40%, 40–50%, 50–60%, and 60–70%, respectively.
These values provide empirical references for the expected reconstruction error under different missing-data conditions.
The empirical RMSE values should not be interpreted as strict pixel-level probabilistic uncertainty bounds.
When using reconstructed SM estimates (source flag = 2), users are advised to consider the corresponding empirical reconstruction error associated with the missing-rate range and to distinguish reconstructed estimates from original observations (source flag = 1) using the source flag."

Page 19, Lines 511-513
"The accuracy metrics of GSP in simulated-gap experiments further provide the uncertainty references when using reconstructed FY-3B SM under the corresponding missing-data conditions."

Page 14, Lines 424-427
"To evaluate the reconstructed FY-3B SM datasets under actual missing-data conditions, two types of in-situ networks, including sparse and dense networks, were employed. The in-situ observations (i.e., 17 sparse networks and five dense networks) were evaluated at locations and dates corresponding to actual missing FY-3B SM observations."

Page 28, Lines 675-681
"Firstly, the proposed GSP framework has a limitation in that its reconstruction relies entirely on the available spatiotemporal information within the FY-3B SM dataset. When the effective neighboring information is substantially reduced, the reconstruction uncertainty may increase. To alleviate this limitation, future studies could consider incorporating heterogeneous auxiliary data, such as precipitation and LST, to provide complementary information and enhance the robustness of GSP under large-scale and continuous missing-data conditions."

Minor comments
1) Fig. 1: The definition of "temporal coverage proportion" should be clearly explained. How can some regions reach 100% coverage for a LEO satellite?

Re: Thank you for this comment. We sincerely thank the reviewer for pointing this out. The temporal coverage proportion of FY-3B LST cannot achieve 100% temporal coverage at a given location due to the discontinuous revisit orbit. The previous "100%" label was an error in color bar scaling. We have corrected Fig 1. As shown in the revised figure, the actual maximum temporal coverage proportion in our dataset is 92.8%. Furthermore, to avoid any ambiguity, we have explicitly added the definition of "temporal coverage proportion" in Page 2, Lines 82-85.

Fig. 1

"

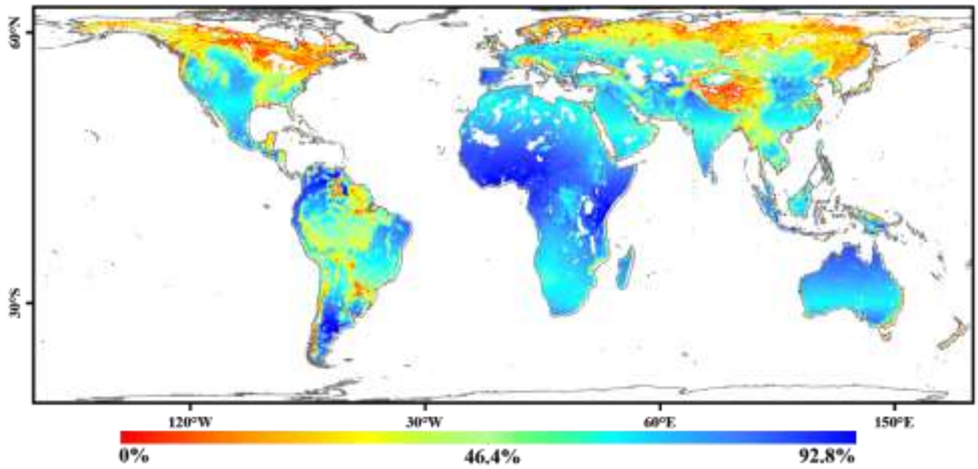

Fig. 1. *The temporal coverage proportion of FY-3B SM at the global scale from 12 July 2011 to 19 August 2019."*

Page 2, Lines 82-85

"

The temporal coverage proportion is defined as the ratio of the number of days with valid satellite retrievals to the total number of days within the study period for each pixel. Due to the discontinuous revisit orbits, the maximum temporal coverage proportion reaches 92.8%. It is seen that the proportion varies spatially, with particularly severe gaps observed in high latitude areas.

"

2) Table 1: The distinction between sparse and dense networks should be clarified. The definition seems to be based on the number of stations within each FY-3B pixel. If this is the case, it would be useful to report the number of matched FY-3B pixels and the average number of stations per pixel, rather than the total number of stations per network.

Re: Thank you for this valuable suggestion. We have clarified the definition of sparse and dense in-situ networks in Page 12, Lines 402-406. Specifically, the classification is based on the spatial distribution of the stations relative to the FY-3B pixels, a network is defined as dense when all stations are located within a single FY-3B pixel, whereas it is defined as sparse when the stations are distributed across multiple FY-3B pixels. We have also added two columns to Table 1, namely, the number of matched FY-3B SM pixels and the average number of stations per pixel. The former indicates the number of FY-3B pixels containing at least one matched in-situ station. The latter is calculated by dividing the total number of stations in each network by the number of matched FY-3B pixels and is rounded to the nearest integer. These additional statistics provide a clearer quantitative description of the spatial concentration of the stations within each network. The corresponding description has been revised in Page 13, Lines 408-411 and Table 1 has been updated accordingly.

Page 12, Lines 402-406

"Meanwhile, to minimize the effects of differences in spatial locations of stations, all networks were divided into two types according to the distribution of stations, including sparse (i.e., stations are distributed across multiple FY-3B SM pixels) and dense (i.e., all stations in a network, which may contain one or more stations, are distributed within a single FY-3B SM pixel) in-situ data."

Page 13, Lines 408-411

"As shown in Table 1, a larger number of matched FY-3B pixels indicates a more spatially dispersed station distribution, whereas a larger average number of stations per pixel indicates a greater concentration of stations within individual FY-3B pixels."

Table 1

"

Types	***Network***	***Number of matched FY-3B SM pixels***	***Average number of stations per pixel***	***Location (country)***	***Period (yyyy/mm/dd)***
Sparse	***AMMA-CATCH***	*3*	*2*	*Benin, Niger, Mali*	*2006/01/01 to 2018/12/31*
	ARM	*20*	*1*	*USA*	*1993/06/29 to 2025/12/14*
	CTP_SMTMN	*11*	*5*	*China*	*2010/08/01 to 2016/09/19*
	MAQU	*9*	*3*	*China*	*2008/05/13 to 2019/06/01*
	NAQU	*3*	*4*	*China*	*2010/06/15 to 2019/09/12*
	ORACLE	*3*	*1*	*France*	*1985/10/18 to 2013/09/09*
	OZNET	*10*	*2*	*Australia*	*2001/09/12 to 2021/09/01*
	PBO_H2O	*123*	*1*	*USA*	*2004/09/27 to 2017/12/16*
	REMEDHUS	*4*	*5*	*Spain*	*2005/03/15 to 2025/01/01*
	SCAN	*188*	*1*	*USA*	*1996/08/15 to 2025/12/16*
	SMN-SDR	*16*	*2*	*China*	*2018/07/25 to 2019/12/31*
	SNOTEL	*270*	*1*	*USA*	*1996/09/10 to 2025/12/16*
	SOILSCAPE	*5*	*21*	*USA*	*2011/08/03 to 2025/12/16*
	TAHMO	*2*	*1*	*Côte d'Ivoire, Nigeria, Ghana, Uganda, Rwanda, Kenya*	*2015/06/17 to 2022/07/07*
	TxSON	*5*	*8*	*USA*	*2014/10/01 to 2022/11/08*
	USCAN	*93*	*1*	*USA*	*2000/11/15 to 2025/12/16*
	XMS-CAT	*4*	*2*	*Spain*	*2016/08/01 to 2025/12/16*
Dense	***BIEBRZA_S-1***	*1*	*30*	*Poland*	*2015/04/23 to 2018/12/01*
	Ru_CFR	*1*	*2*	*Russia*	*2015/05/25 to 2024/12/31*
	SD_DEM	*1*	*1*	*Sudan*	*2002/02/08 to 2020/11/12*

SWEX_POLAND	*1*	*6*	*Poland*	*2000/01/01 to 2013/05/06*
VAS	*1*	*3*	*Spain*	*2010/01/01 to 2012/01/01*

”

3) The manuscript contains too many figures and tables with overlapping messages. Figs. 5–6 and Tables 2–3 all present in-situ validation. Figs. 7–10 and Table 4 also convey the same simulated gap evaluation and do not provide different messages. Fig. 12 is merely a sequence of images. Many of these materials could be summarized into a figure/table or moved to the supplement.

Re: Thank you for this valuable suggestion. We agree that some of the figures and tables in the original manuscript conveyed related information, and we have therefore carefully reconsidered their presentation to reduce redundancy and improve the readability of the manuscript. Regarding Figs. 5–6 (in the original manuscript) and Tables 2–3, although all four present in-situ validation results, they correspond to two different types of station networks. Specifically, Fig. 5(in the original manuscript) and Table 2 present the results for sparse networks, whereas Fig. 6 (in the original manuscript) and Table 3 present the results for dense networks. This separation was designed to minimize the effects of differences in spatial locations of stations and to evaluate the reconstruction under different station-distribution conditions. In addition, the dense-network evaluation includes a comparison with the original FY-3B SM, which provides an additional reference for assessing whether the reconstructed dataset can preserve the characteristics of the original product. Therefore, these two sets of results provide complementary information rather than simply repeating the same evaluation. For Figs. 7–10 (in the original manuscript) and Table 4, the four figures correspond to simulated missing-data rates of 30%–40%, 40%–50%, 50%–60%, and 60%–70%, respectively. These figures are primarily intended to provide a visual and qualitative comparison of the reconstructed spatial results by different methods under different missing-data conditions. In contrast, Table 4 provides a quantitative and comprehensive evaluation of the reconstruction accuracy using statistical metrics across the different missing-data scenarios. Thus, the figures and table provide complementary qualitative and quantitative assessments. Following the reviewer’s suggestion, we have reduced the amount of material presented in the main text by moving the results for the 30%–40% and 40%–50% missing-data scenarios (Figs. 7 and 8, in the original manuscript) to the Supplementary Material (Page 18, Lines 494-498). Additionally, we agree that the original Fig. 12 (in the original manuscript), which mainly presented the reconstructed FY-3B SM over a continuous 30-day period, provided limited information for assessing the temporal and spatial variability of the reconstructed dataset. Therefore, we substantially redesigned this analysis in the revised manuscript. The revised Fig. 12 (in the revised version) now provides a more comprehensive characterization of the reconstructed FY-3B SM during September 2015. Specifically, four representative daily reconstructed SM maps are presented to illustrate the continuous spatial evolution during the month. In addition, the monthly mean and temporal standard deviation of the reconstructed FY-3B SM and precipitation are calculated to characterize its overall spatial distribution and temporal variability and examine whether the physical meaning of the reconstructed FY-3B SM based on GSP. The detailed description can be found on Page 24, Lines 546-557.

Page 18, Lines 494-498

“Figs. 9–10 present the spatial distributions of the original and reconstructed FY-3B SM under

missing proportions ranging from 50% to 70%, with six randomly selected patches shown for each scenario. Additional results for missing proportions ranging from 30% to 50% are presented in Appendix A.1 and Appendix A.2, where six randomly selected patches are shown for each scenario."

Page 24, Lines 546-557

"Furthermore, Fig. 12 illustrates the spatial patterns of the reconstructed FY-3B SM and precipitation. (a)–(d) demonstrate that the reconstructed results maintain a consistent spatial structure while exhibiting certain variations, indicating the model's capability to capture continuous daily evolutions. Furthermore, the monthly mean of reconstructed FY-3B SM (Fig. 12 (e)) falls within a physically reasonable range of 0 to 0.5 m^3/m^3, and the standard deviation (Fig. 12 (f)) is constrained within 0 to 0.16 m^3/m^3. These quantitative results demonstrate that the overall spatial configuration remains stable, alongside the presence of localized daily fluctuations. To validate the physical rationale behind the reconstructed FY-3B SM dynamics, we introduced the monthly mean and standard deviation of precipitation for the same period (Fig. 12 (g)–(h)). It is evident that regions with a higher FY-3B SM standard deviation are spatially consistent with active precipitation zones. This consistency confirms that the GSP accurately captures the dynamic hydrological responses."

Fig. 12

"

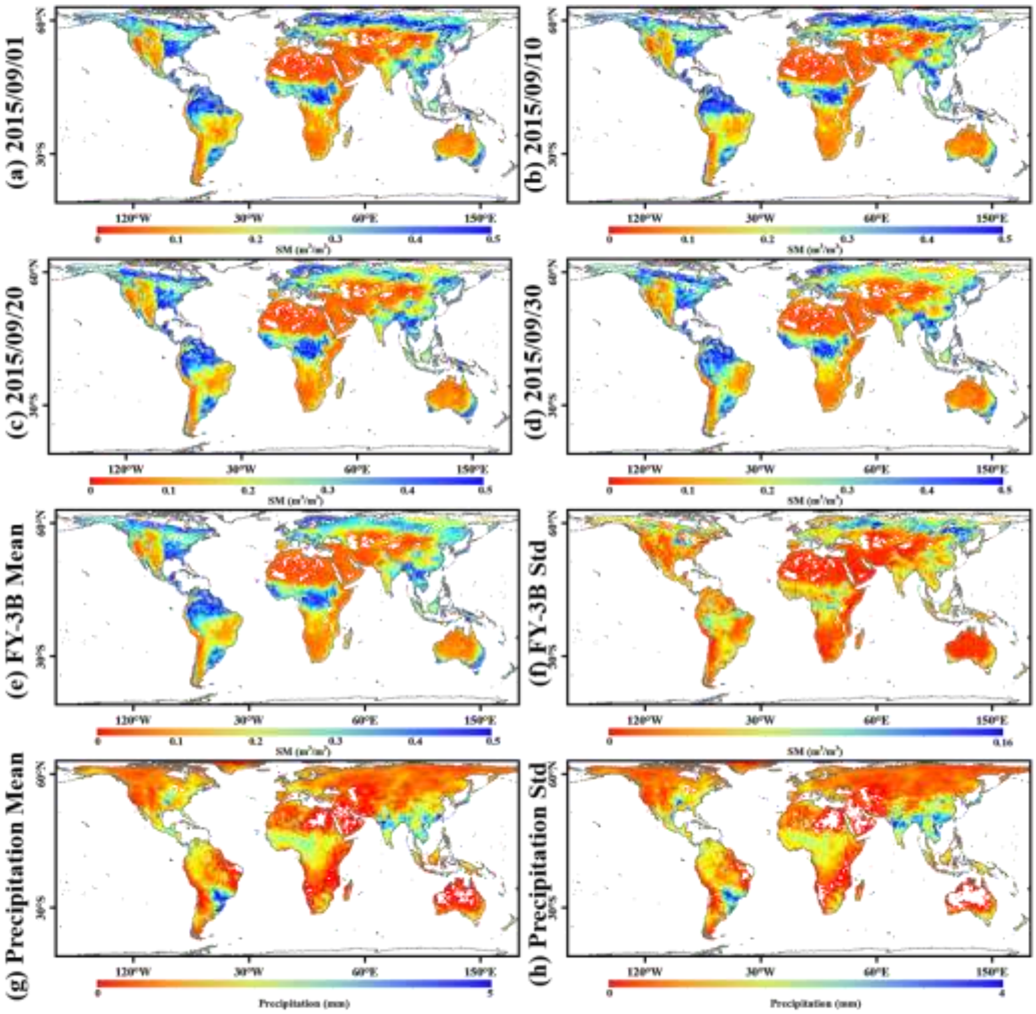

Fig. 12. *Spatial distributions of the reconstructed FY-3B SM and precipitation in September 2015. (a)–(d) present daily reconstructed FY-3B SM on 1 September 2015, 10 September 2015, 20 September 2015, and 30 September 2015, respectively. (e)–(f) present the monthly mean and temporal standard deviation of FY-3B SM for the September 2015. (g)–(h) present the monthly mean and STD of precipitation for the same period.*

”

4) The visual comparisons between soil moisture products are not always convincing. For example, several patch-level figures show similar soil moisture patterns, so it is difficult to judge whether GSP is truly better. Difference maps would be more informative than absolute maps alone.

Re: Thank you very much for this valuable comment. Since GLDAS-Noah is a land surface model product with certain uncertainty, it is no longer treated as a truth reference for evaluating reconstruction accuracy. Instead, GLDAS-Noah is retained only as an independent comparison dataset for examining large-scale spatial characteristics. The regional spatial maps in Fig. 16(c) were retained to illustrate the overall spatial structures and local textures of the reconstructed datasets. Because no dataset is regarded as a reference in this comparison, regional difference maps relative to selected patches were not included. Following the reviewer’s suggestion, we further revised Fig. 16(b) to more explicitly highlight the differences between the two reconstructed FY-3B SM datasets. Specifically, the difference between the GSP- and TTP-reconstructed FY-3B SM was additionally calculated and presented together with their spatial variation profiles. This comparison more clearly reveals the discrepancies between the two reconstruction methods within regions where the original FY-3B SM is unavailable. In these missing-data regions, the TTP-reconstructed FY-3B SM tend to be relatively homogeneous and show limited spatial variability, whereas the GSP-reconstructed FY-3B SM exhibits more distinct spatial fluctuations. The variation pattern of the GSP–TTP difference closely follows that of GSP, suggesting that the spatial variability represented by the difference is mainly associated with the additional spatial variation retained by GSP. These results indicate that incorporating surrounding spatial information enables GSP to better preserve the spatial variability of FY-3B SM during reconstruction. We have revised Fig. 14 and added the following detailed discussion to Page 24, Lines 593–619 to explicitly analyze the difference maps.

Fig. 14

“

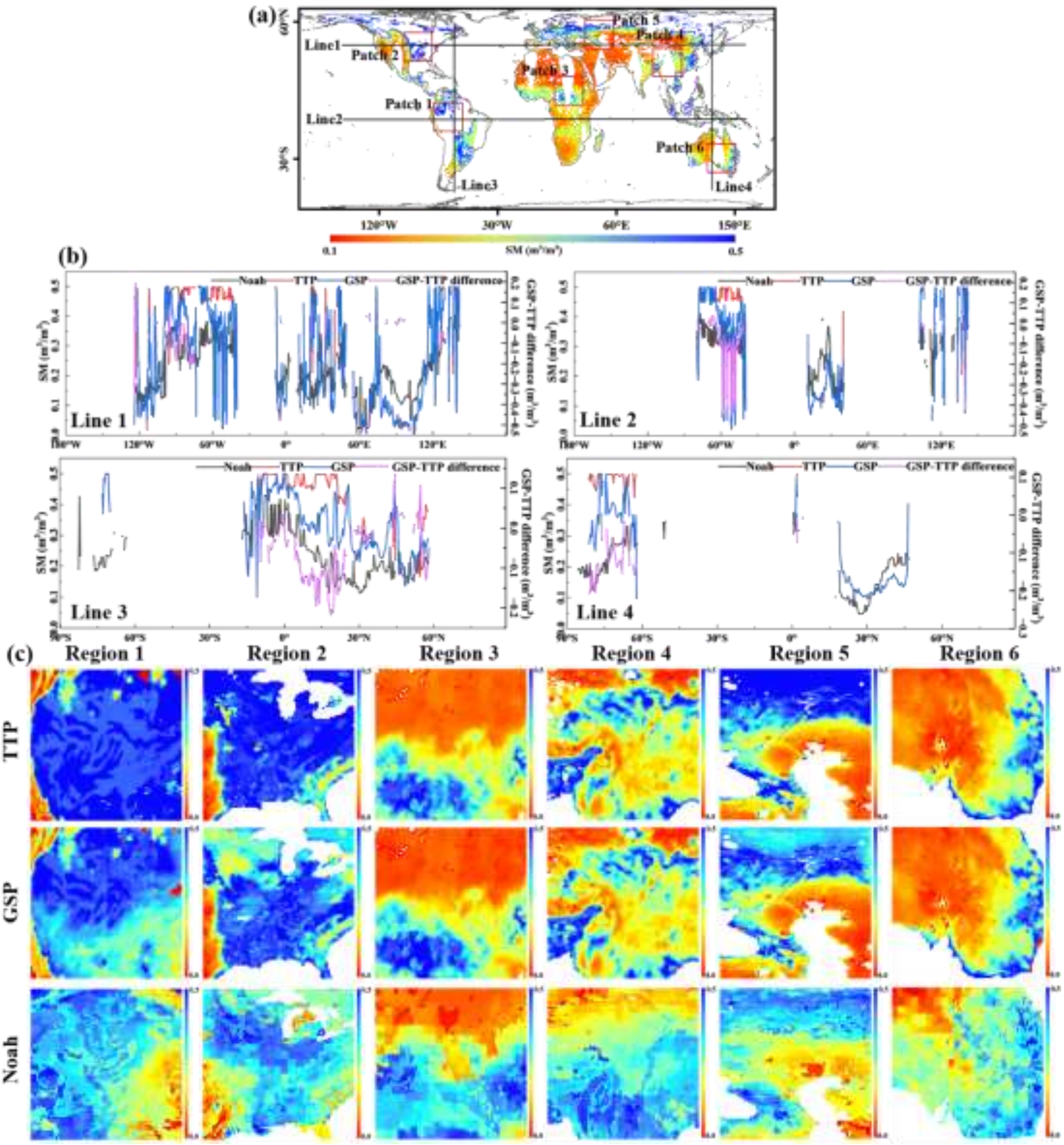

Fig. 14. Comparison of spatial heterogeneity among the TTP-reconstructed FY-3B SM, GSP-reconstructed FY-3B SM, and GLDAS-Noah SM. (a) Locations of six randomly selected patches and four lines at the global scale, where the four lines include two horizontal lines at 41.2485° N and 3.0274° S, and two longitudinal lines at 62.9935° W and 132.2343° E. The center coordinates of the six patches are Region 1 (4.0054° S, 67.4187° W), Region 2 (37.7069° N, 88.2429° W), Region 3 (11.6971° N, 26.2907° E), Region 4 (28.3807° N, 99.1757° E), Region 5 (48.4103° N, 47.1150° E), and Region 6 (28.6028° S, 140.8243° E). (b) Spatial variation profiles of SM along the four lines, comparing TTP-reconstructed FY-3B SM, GSP-reconstructed FY-3B SM, and GLDAS-Noah SM. (c) Visual comparison of the spatial SM patterns of the TTP-reconstructed FY-3B SM, GSP-reconstructed FY-3B SM, and GLDAS-Noah SM for the six selected patches.

”

Page 24, Lines 593–619

"5.3 Spatial comparison among the GSP- and TTP-reconstructed FY-3B SM datasets and GLDAS-Noah SM

To further examine the spatial characteristics of the reconstructed FY-3B SM dataset, the 25 km GLDAS-Noah SM dataset, which provides spatially complete SM estimates, was introduced as a comparison dataset. Taking the GLDAS-Noah SM dataset and TTP- and GSP-reconstructed FY-3B SM on 16 July 2011 as an example, four lines and six patches were randomly selected for spatial comparison, as shown in Fig. 14. As shown in Fig. 14(b), the TTP-reconstructed FY-3B SM exhibits very limited spatial variation, with locally nearly invariant SM. In contrast, the GSP-reconstructed FY-3B SM shows more pronounced spatial variations. The variation pattern of the difference between GSP and TTP is also generally consistent with that of GSP, indicating that much of the spatial variation between the two reconstructed datasets originates from the spatial variability retained by GSP, whereas the TTP reconstruction tends to produce a more spatially homogeneous distribution. Moreover, the spatial variation patterns of GSP and GLDAS-Noah show broadly consistent fluctuations along several transects. A similar pattern can be observed from the spatial maps in Fig. 14(c). The TTP-reconstructed FY-3B SM exhibits relatively weak spatial texture, whereas the GSP-reconstructed results present more continuous and complete spatial structures while retaining finer spatial details. GLDAS-Noah also reproduces the major large-scale spatial variations, but appears relatively smooth in some regions. This is likely related to the nature of GLDAS-Noah as a land surface model product, for which the spatial distribution is influenced by meteorological forcing, model parameterization, and grid-scale averaging, thereby smoothing part of the local-scale spatial heterogeneity. These comparisons further indicate that, compared with TTP, which primarily considers temporal relationships, GSP can better preserve and reconstruct the spatial structure of the original FY-3B SM by incorporating information from the surrounding spatiotemporal neighborhood. Meanwhile, compared with the model-based GLDAS-Noah dataset, the GSP-reconstructed FY-3B SM based on satellite SM retains more localized spatial details in some regions, reflecting the spatial characteristics inherited from the original satellite observations.

5) Please carefully check types. For example, in lines 261-263, "form" should be "from". In line 383, "FY-3M" should be "FY-3B". At line 497, 1 February 2011 is outside the study period.

Re: Thank you for carefully pointing out these typographical and consistency issues. We have thoroughly checked the manuscript and corrected all the indicated errors. We have also carefully proofread the manuscript to identify and correct similar typographical errors and inconsistencies throughout the revised manuscript. The corresponding corrections can be found on Page 7, Lines 273–276, Page 14, Lines 428–429, and Page 21, Lines 541–543 of the revised manuscript.

Page 7, Lines 273–276

"It should be noted that, for the special case of periods without sufficient earlier (or later) FY-3B SM data, that is, from 12 July 2011 to 15 July 2011 (16 August 2019 to 19 August 2019), the FY-3B SM data from T *to* $T+4$ *(from* $T-4$ *to* T*) are used as input for the model (i.e., treat the data from* $T-4$ *to* $T-1$ *(from* $T+1$ *to* $T+4$*) as completely missing data).*

"

Page 14, Lines 428–429

"In the validation based on the in-situ data at the sparse networks, the 17 sparse networks were used to evaluate the accuracy of the seamless FY-3B dataset generated by different methods."

Page 21, Lines 541–543

"Fig. 11 shows the original and reconstructed FY-3B SM on five randomly selected dates (i.e., 1 October 2011, 1 August 2013, 1 June 2015, 1 April 2017, and 1 February 2019)."